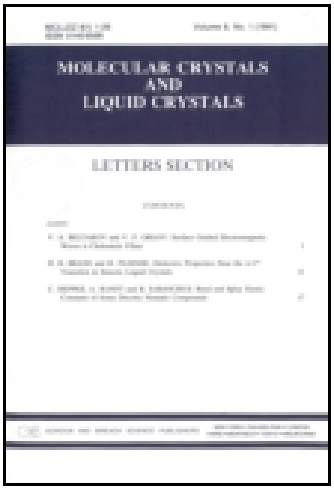

Molecular Crystals and Liquid Crystals
Publication details, including instructions for authors and subscription information:
http://www.tandfonline.com/loi/gmcl20

Processes of Encapsulation and Crystallization of Prednisolon in PAAm-b-PEO-b-PAAm Micellar Solutions

Tatyana Zheltonozhskaya [a], Sofia Partsevskaya [a], Vasil Gorchev [b] & Dmytro Klymchuk [c]

[a] Taras Shevchenko National University of Kiev, Faculty of Chemistry, Department of Macromolecular Chemistry, 60 Vladimirskaya St, 01033, Kiev, Ukraine

[b] Institute of Biochemistry, National Academy of Sciences of Ukraine, 9 Leontovycha St, 01601, Kiev, Ukraine

[c] Institute of Botany, National Academy of Sciences of Ukraine, 2 Tereschenkovskaya St., 01601, Kiev, Ukraine

Published online: 28 Mar 2014.

To cite this article: Tatyana Zheltonozhskaya, Sofia Partsevskaya, Vasil Gorchev & Dmytro Klymchuk (2014) Processes of Encapsulation and Crystallization of Prednisolon in PAAm-b-PEO-b-PAAm Micellar Solutions, Molecular Crystals and Liquid Crystals, 590:1, 140-148, DOI: 10.1080/15421406.2013.874155

To link to this article: http://dx.doi.org/10.1080/15421406.2013.874155

Mol. Cryst. Liq. Cryst., Vol. 590: pp. 140–148, 2014

ISSN: 1542-1406 print/1563-5287 online
DOI: 10.1080/15421406.2013.874155

Processes of Encapsulation and Crystallization of Prednisolon in PAAm-*b*-PEO-*b*-PAAm Micellar Solutions

TATYANA ZHELTONOZHSKAYA,[1,*]
SOFIA PARTSEVSKAYA,[1] VASIL GORCHEV,[2]
AND DMYTRO KLYMCHUK[3]

[1]Taras Shevchenko National University of Kiev, Faculty of Chemistry, Department of Macromolecular Chemistry, 60 Vladimirskaya St 01033, Kiev, Ukraine
[2]Institute of Biochemistry, National Academy of Sciences of Ukraine, 9 Leontovycha St 01601, Kiev, Ukraine
[3]Institute of Botany, National Academy of Sciences of Ukraine, 2 Tereschenkovskaya St. 01601, Kiev, Ukraine

Micellar solutions of PAAm-b-*PEO*-b-*PAAm triblock copolymer (TBC) based on chemically complementary poly(ethylene oxide) and polyacrylamide ($M_n = 6$ and 116 kDa) were applied to study the encapsulation of poorly soluble crystallizing drug prednisolon (PS) in a region of $\varphi = 0.065 \div 0.39$ mol_{PS}/base-mol_{TBC}. The equilibrium mechanism of the encapsulation and the effect of specific aggregation of small and large PS-loaded micelles by their "coronas" that promoted the drug crystallization were established. The fractal character of large drug-loaded micelles and unusual morphology of PS crystals allowed assuming the presence of TBC micelles inside crystalline space.*

Keywords Triblock copolymer; intramolecular polycomplex; monomolecular-type and polymolecular-type micelles; prednisolon; encapsulation.

Introduction

Polymeric micelles or micellar nanocontainers are perspective vehicles for passive and active (targeted or intracellular) delivery of toxic and poorly soluble drugs and also biopolymers in living organisms [1–5]. They allow creating water-soluble forms of poorly soluble drugs due to encapsulation of their molecules into micellar "core," intermediate layer or "corona," ensuring long-term circulation and controlled release of drugs in the blood stream by regulation of the drug carrier size and building, preventing a rapid drug degradation in fermentative and metabolisms processes, protecting healthy organs and tissues of living organisms from a destructive action of toxic drugs, in particular, at the chemotherapy [2,6–10].

We showed earlier [11] that one of the simplest ways to create micellar nanocontainers, which ones: i) contain a complex "core," ii) possess high binding capability with respect

*Address correspondence to Tatyana Zheltonozhskaya. Tel.: +380442393411, Fax: 3804423-93100. E-mail: zheltonozhskaya@ukr.net

to toxic poorly soluble drugs (similar to a model drug prednisolon, PS), and iii) could not be destructed up to individual components in any competitive processes, is a self-assembly of asymmetric block copolymers with hydrophilic chemically complementary blocks. In this context, the micellization of asymmetric triblock copolymers (TBCs) comprised chemically complementary poly(ethylene oxide) and polyacrylamide of different chain length (PAAm-*b*-PEO-*b*-PAAm) was studied and the formation of "hairy-type" micelles in aqueous solutions was established. Significant encapsulation of a crystalline drug PS by TBC micelles due to hydrogen bonds and hydrophobic interactions resulted in the appearance of "snow-flakes-like" micellar structures [11].

In this work, the additional studies of PS encapsulation by TBC micelles were performed using dynamic light scattering (DLS) and transmission electron microscopy (TEM) in order to display the mechanism of PS encapsulation, the nature of "snow-flakes-like" structures and the role of TBC micelles in PS crystallization.

Experimental

A sample of PAAm-*b*-PEO-*b*-PAAm triblock copolymer was obtained by a matrix free-radical block copolymerization of acrylamide from "Merk" (Germany) with poly(ethylene glycol) of molecular weight $M_{nPEG} = 6.0$ kDa from "Aldrich" (USA). Ammonium cerium (IV) nitrate from the last firm was used as initiator. Detail synthesis scheme and matrix mechanism of the copolymerization process were described elsewhere [12,13]. Chemical structure of TBC was confirmed and the molecular weight of PAAm blocks ($M_{nPAAm} =$ 116 kDa) was determined using ^{1}H NMR spectroscopy as in the study [11]. The molecular weight of TBC sample calculated by the formula: $M_{nTBC} = M_{nPEO} + 2 \cdot M_{nPAAm}$ was equal to 238 kDa. The sample of commercial crystalline PS from "Sigma Aldrich" (USA) was also used in our studies.

The compositions of PS with TBC micelles were prepared at the constant copolymer concentration (0.3 and 0.5 $kg \cdot m^{-3}$ consequently for DLS and TEM experiments) and a variable concentration of the drug (from 0.09 to 0.55 $kg \cdot m^{-3}$). The selected TBC concentrations were higher than the critical micellization concentration (CMC = 0.09 $kg \cdot m^{-3}$ [11]) but in some times less than that (1 $kg \cdot m^{-3}$) used earlier to characterize the PS encapsulation degree [11]. Also, the range of PS/TBC contents studied in DLS experiments ($\varphi = 0.065 \div 0.39$ mol_{PS}/base-mol_{TBC}) did not include large values of $\varphi = 0.42$ and 0.60, at which a quick formation of the "snow-flakes-like" structures occurred [11]. Thus, PS encapsulation and its consequences could be clearly controlled. A small volume of PS ethanol solution (10 v/%) was added to a large volume of TBC solution in dusty-free deionized water at the blending to ensure homogeneous mixing of the components. All the researchers were carried out in 24 h after mixing. Additionally, the same portions of PS ethanol solutions were introduced into corresponding volumes of the copolymer-free deionized water to study the behavior of pure PS. The drug-free aqueous solutions of TBC were studied also.

DLS experiments were performed with a ZetaSizer 3 instrument ("Malvern," UK) using a He-Ne laser operating at $\lambda = 632.8$ nm as a light source. In every solution, 10-12 parallel measurements of the autocorrelation function were carried out. The results were analyzed by the monomodal distribution approach and CONTIN algorithm (PCS program: size mode v.1.61). The last processing allowed obtaining also the size distributions based on particle volumes, which reflected more adequately a situation in different solutions and gave more precise average diameters of scattering particles.

TEM images of the copolymer micelles before and after PS introduction were recorded with a JEM-1230 instrument ("JEOL," Japan) operating at an accelerating voltage of 90 kV. Small drops ($\sim 1 \cdot 10^{-4}$ cm^3) of TBC solutions or PS/TBC compositions with $\varphi = 0.2$ mol$_{PS}$/base-mol$_{TBC}$ were deposited in copper grids coated with Formvar film and carbon and then were dried for $\sim$1 min at 20°C. Electronic images were recorded in one day after the sample preparation.

Results and Discussion

The driving forces of TBC micellization in dilute aqueous solutions such as: i) formation of the intramolecular polycomplexes (IntraPCs) in individual TBC macromolecules due to hydrogen bonding chemically complementary PAAm and PEO blocks, and ii) segregation of hydrophobic bound parts of both the blocks in water medium (in fact, hydrophobic aggregation of some IntraPCs) were discussed earlier [11,12]. Based on highly asymmetric character of TBC blocks, the appearance of "hairy-type" micelles of spherical shape has been assumed. Indeed, TEM images in Fig. 1, especially image **b**, demonstrated mainly spherical micellar structures with common "core" and developed "corona," which diameter changed from 80 to 240 nm. It is clear that these micelles belong to the polymolecular-type (PMMs).

The image in Fig. 1**b** shows additionally numerous dark points with a size in the range of 15 ÷ 30 nm and also separate aggregates of large PMMs, which dimensions are higher than 240 nm. Taking into account a special building of individual TBC macromolecules, we attributed dark points in this image to separate IntraPCs, which are in fact the

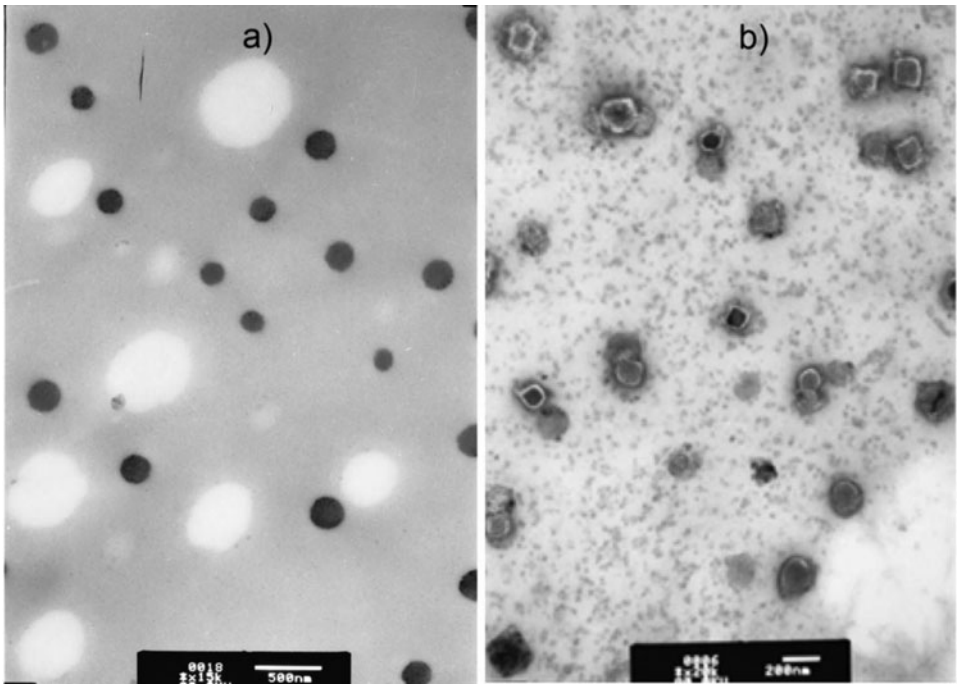

Figure 1. TEM images of (**a**) polymolecular micelles and (**b**) mono- and polymolecular micelles of TBC. C = 0.2 kg·m^{-3}, T = 20 °C.

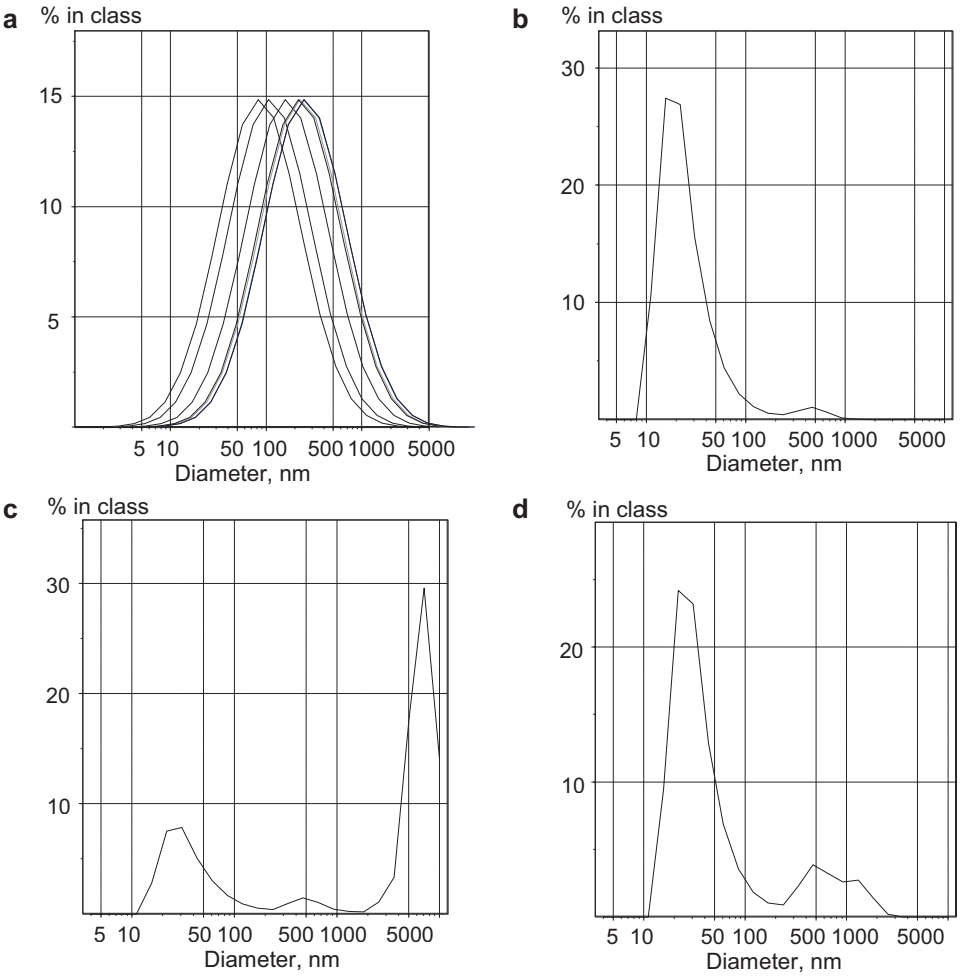

Figure 2. The examples of size distributions based on (**a**) scattering intensities and (**b**, **c**, **d**) particle volumes for (**a**, **b**) TBC solutions and (**c**, **d**) PS/TBC compositions at $\varphi = 0.065$ (**c**) and 0.13 (**d**) mol_{PS}/base-mol_{TBC}. $C_{TBC} = 0.3$ kg·m^{-3}, T = 20°C.

monomolecular-type micelles (MMMs) [14]. In this context, the results of DLS researchers of the drug-free TBC solutions, which are represented in Fig. 2 (**a**, **b**) and Table 1, are of special interest.

The most important result is a bimodal size distribution based on particle volume (Fig. 2**b**), which has been established by CONTIN processing. This result confirmed the existence in TBC solution a large quantity (97.1 v/%) of small scattering particles (MMMs) with the average diameter $d_{av(v)} = 28$ nm and some quantity (2.9 v/%) of large scattering particles (PMMs and their aggregates) with $d_{av(v)} = 468$ nm (Table 1).

A state of PS molecules in water/ethanol (90/10 v/v) solutions at different drug concentrations is characterized by DLS data in Table 2. The bimodal size distributions based not only on particle volume but also on the scattering intensity were observed in the most cases (at the most concentrations of this poorly soluble drug excluding $C_{PS} = 0.274$ and partially 0.366 kg·m^{-3}). Thus, two types of aggregates with essentially different size existed in the

Table 1. The effect of PS encapsulation on a state and size of the triblock copolymer micelles

System	C_{PS}, kg·m^{-3}	φ, mol/ base-mol	d_{av} [1] nm	$d_{min} \div d_{max}$ [2] nm	$d_{av(i)}$ [3] nm	$X_{(i)}$ [4] %	$d_{av(v)}$ [3] nm	$X_{(v)}$ [4] %	$d_{av(n)}$ [3] nm
TBC	—	—	109	16 ÷ 924	218	100	28	97.1	18
							468	2.9	
PS/TBC	0.092	0.065	254	22 ÷ 1299	309	80.0	43	29.6	26
				2565 ÷ 7116	5743	20.0	601	4.7	
							6912	65.7	
	0.183	0.130	163	22 ÷ 1825	443	100	39	81.0	25
							567	12.4	
							1299	6.6	
	0.274	0.195	85	11 ÷ 61	30	11.1	16	96.7	12
				61 ÷ 1299	496	88.9	670	3.3	
	0.366	0.260	232	22 ÷ 658	181	60.2	37	31.4	25
				1825 ÷ 7116	5306	39.8	468	1.0	
							6738	67.6	
	0.550	0.390	255	22 ÷ 658	198	73.7	40	37.0	26
				1825 ÷ 10000	5485	26.3	442	1.8	
							6815	61.2	

[1] The average particle diameter based on scattering intensities and the monomodal distribution approach.
[2] The range of particle dimensions in corresponding distribution.
[3] The average particle diameters based on scattering intensities, particle volume and particle number consequently (the results of CONTIN processing).
[4] The contribution of separate modes into the whole size distributions based on scattering intensity and particle size, correspondingly.

Table 2. Aggregation of prednisolon molecules in water at small ethanol content [1]

System	C, kg·m^{-3}	$d_{min} \div d_{max}$, nm	$d_{av(i)}$, nm	$X_{(i)}$, %	$d_{av(v)}$, nm	$X_{(v)}$, %	$d_{av(n)}$, nm
PS	0.092	9 ÷ 102	42	27.4	14	98.1	10
		595 ÷ 2440	1575	72.6	1828	1.9	
	0.183	14 ÷ 51	25	5.4	18	81.6	15
		264 ÷ 1916	1002	94.6	1185	18.4	
	0.274	37 ÷ 9143	2906	100	5968	99.9	46
	0.366	21 ÷ 13945	4076	100	40	1.5	25
					7741	98.5	
	0.458	21 ÷ 111	41	4.1	27	20.2	24
		576 ÷ 9009	4603	95.9	6166	79.8	
	0.550	15 ÷ 44	26	5.4	19	79	16
		379 ÷ 3296	1600	94.6	1923	21	

[1] Ethanol content is in all the cases 10 v/%.

solutions of pure PS. At the smallest PS concentration, the majority of its molecules formed small aggregates with the average diameter $d_{av(v)} = 14$ nm (Table 2). It is not surprising taking into account a weak solubility of the drug in pure water (0.27 mg·cm^{-3}) and water/ethanol 90/10 v/v solutions (0.62 mg·cm^{-3}) [15]. With increasing PS concentration up to 0.366 kg·m^{-3}, the size of small aggregates rose and their relative quantity diminished while the quantity and size of large aggregates grew. The diametrically opposite tendency was observed at further increase in PS concentration up to 0.55 kg·m^{-3} (Table 2). The size and relative quantity of small aggregates correspondingly decrease and rose, while both the parameters for large aggregates diminished. The last tendency could be explained by a partial precipitation of very large PS aggregates at $C_{PS} > 0.366$ kg·m^{-3}. Actually, a very weak turbidity appeared in PS solutions with $C_{PS} = 0.458$ and 0.55 kg·m^{-3} in 24 hours' time unlike other PS solutions, which were absolutely transparent during this time. The above-mentioned facts pointed out the existence of a dynamic equilibrium between small and large PS aggregates in the mixed solvent that was dependent on the drug concentration.

The nature of PS encapsulation into TBC micelles (by hydrogen bonds and hydrophobic interactions) was detail considered earlier [11]. The blocks of PAAm were shown to be essentially more active in respect of PS connection than PEO blocks. At the interaction with PAAm chains, not only hydroxyl groups but also carbonyl groups of PS molecules participated in their binding. This allows assuming that the encapsulation process developed mainly in the "coronas" of TBC micelles, which were formed by the surplus (unbound with PEO) PAAm segments [11]. Let's consider from such point of view the results of DLS investigations of PS/TBC compositions represented in Fig. 2(**c**, **d**) and Table 1. It should be noted that all PS/TBC compositions in the studied φ region were transparent in 24 hours' time.

The size distributions based on particle volumes, which were obtained for the first two PS/TBC contents (Fig. 2**c**, **d**), demonstrated three modes that is three different types of scattering particles. One is reasonable to attribute two of them with less $d_{av(v)}$ values (Table 1) to the drug-containing MMMs and PMMs. The appearance of third-type scattering particles, which contribution and dimension essentially decreased and reached to zero at φ growth up to 0.195, could be explained by: i) the development of the encapsulation process according to the equilibrium mechanism (the higher relative PS concentration, the higher binding with TBC micelles), and ii) the existence of a real competition between the processes of PS encapsulation and aggregation. Indeed, $d_{av(v)}$ values for the third-type scattering particles in Table 1 were commensurable with those for large PS aggregates (Table 2). When the relative PS content had the smallest value ($\varphi = 0.065$), the aggregation process strongly competed with PS binding; therefore, free large PS aggregates could be identified in a solution. At further increase in PS content up to $\varphi = 0.195$, the process of PS encapsulation became gradually predominant that resulted in a practical disappearance of large PS aggregates. From such point of view, a content of $\varphi = 0.195$ would correspond to a practically full connection of the drug molecules with TBC micelles (to a micelle saturation by PS molecules).

Let's consider in this context TEM images obtained for PS/TBC composition with $\varphi = 0.2$ (Fig. 3**a**–**e**). They proved the presence both the small and large micellar structures, which sizes changed correspondingly in the regions of 16÷200 and 470 ÷ 2400 nm (from the data of Fig. 3**a**,**c**). Moreover, they revealed the phenomenon of strong aggregation of the majority of small and large drug-loaded micelles by their "coronas," which one especially actively developed at the composition drying (because initial PS/TBC solutions were absolutely transparent) and resulted in the formation of PS crystals together with micelles (Fig. 3**a**,**d**). This interesting effect is not unexpected taking into consideration the

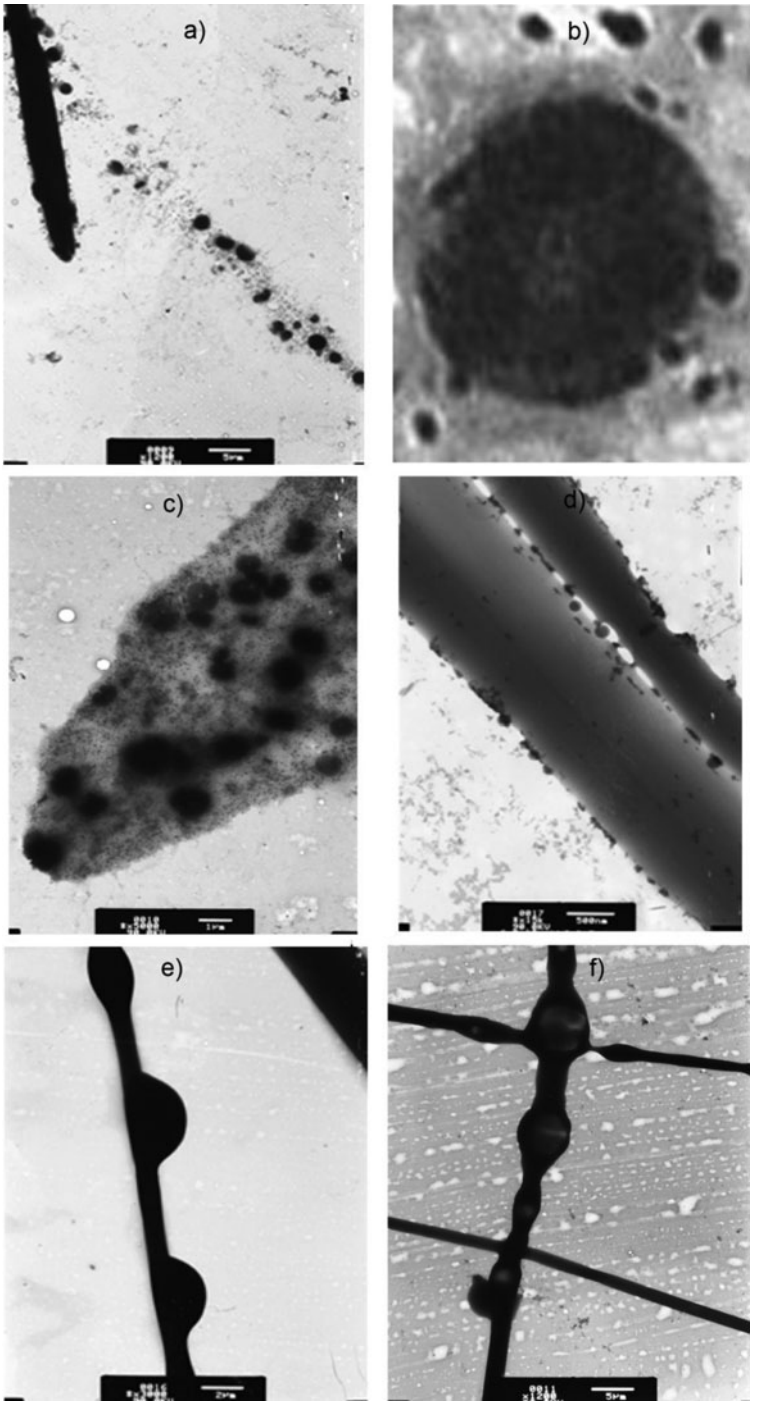

Figure 3. TEM images of: (**a–d**) specific aggregation and crystallization of PS-loaded micelles, (**b**) a large PS-loaded TBC micelle composed of numerous small ones, (**d**) PS crystals with deformed micelles at their surface, and (**e, f**) unusual morphology of crystals in PS/TBC compositions. $C_{TBC} = 0.5$ kg·m^{-3}; $\varphi = 0.2$ (**a–e**) and 0.4 (**f**) mol$_{PS}$/base-mol$_{TBC}$.

above-mentioned preferential connection of the poorly soluble crystallizing PS with PAAm blocks in micellar "coronas." The question about the presence of TBC micelles inside PS crystals but not only on their surface (Fig. 3**c**) is essentially more important. The same TEM images **a, c** but strongly increased showed the presence in the large mainly spherical micelles numerous small micelles, which were connected with each other and formed a regulated fractal structure (one example is shown in Fig. 3**b**). This result allows assuming that PS crystallization developed at the composition drying between micellar "cores" and led to including small TBC micelles (in fact, the drug-loaded IntraPCs) in a crystal space. Due to this, an unusual crystal morphology, which is non-characteristic for the crystals of pure PS [16], arose. Two examples are shown in TEM images for PS/TBC compositions with $\varphi = 0.2$ and 0.4 (Fig. 1**e**,**f**). Thus, specific interactions of the PS-loaded TBC micelles promoted the drug crystallization.

In a region of $\varphi > 0.195$, a sharp increase in the scattering intensity of PS/TBC compositions and the displaying a third mode in the size distributions based on particle volumes took place (Table 1). The appearance of third-type scattering particles of a great size in this φ region is evidently conditioned by strengthening of micelle aggregation due to participation of the surplus PS molecules non-connected directly with TBC micelles.

The alterations in $d_{av(v)}$ values for the small drug-containing TBC micelles at φ growth are not monotonous (Table 1). An initial increase in $d_{av(v)}$ from 28 nm (the average diameter of MMMs in pure water) to 43 nm at $\varphi = 0.065$ is replaced by a gradual reduction in the value up to 16 nm at $\varphi = 0.195$ followed by its growth to the constant number $\sim$ 37–40 nm at further enhance in φ to 0.39. Taking into account the enhanced capability of the PS-loaded micelles to aggregate, we could not attribute the described alterations to changes in the IntraPC state only (to swelling or contraction). But we fixed by TEM some changes in micelle morphology: from mainly spherical shape for MMMs in the solutions of pure TBC to preferentially spheroidal (or ellipsoidal) shape for small drug-loaded TBC micelles at $\varphi = 0.2$ (Fig. 3**a–c**).

Conclusions

Thus, the monomolecular-type and polymolecular-type micelles of essentially different size were found in TBC dilute aqueous solutions at the concentration exceeding CMC. This fact has been confirmed by both TEM and DLS methods. The drug molecules formed in water/ethanol (90/10 v/v) solutions small and large aggregates, which were in a dynamic equilibrium with each other. The encapsulation of PS was shown to develop in the same water/ethanol medium according to equilibrium mechanism (because of existence a real competition between the processes of drug encapsulation and aggregation) and resulted in interesting effects. The main effect consisted in a strong specific aggregation of the drug-loaded micelles by their "coronas" that was especially clearly observed in TEM images and was natural from the point of view the connection of drug molecules mainly with the "corona"-forming PAAm chains. The appearance of large spherical drug-loaded copolymer micelles with fractal-organized structure (comprised numerous small drug-loaded micelles) and the drug crystallization with micelle participation were the consequences of such specific aggregation.

References

[1] Gaucher, G., Dufresne, M.-H., Sant, V. P., Kang, N., Maysinger, D., & Leroux, J.-C. (2005). *J. Contr. Release*, *109*, 169.

[2] Kwon, G. S., & Kataoka, K. (1995). *Adv. Drug Delivery Rev.*, *16*, 295.
[3] Motornov, M., Roiter, Y., Tokarev, I., & Minko, S. (2010). *Prog. Polym. Sci.*, *35*, 174.
[4] Cayre, O. J., Chagneux, N., & Biggs, S. (2011). *Soft Matter*, *7*, 2211.
[5] Ohya, Y., Takahashi, A., & Nagahama, K. (2012). *Adv. Polym. Sci.*, *247*, 65.
[6] Kwon, G. S., & Forrest, M. L. (2006). *Drug Dev. Res.*, *67*, 15.
[7] Miller, A. C., Bershteyn, A., Tan, W., Hammond, P. T., Cohen, R. E., & Irvine, D. J. (2009). *Biomacromolecules*, *10*, 732.
[8] Kim, J. O., Kabanov, A. V., & Bronich, T. K. (2009) *J. Contr. Release*, *138*, 197.
[9] Attia, A. B. E., Ong, Z. Y., Hedrick, J. L., Lee, P. P., Ee, P. L. R., Hammond, P. T., & Yang, Y.-Y. (2011). *Curr. Opinion Coll. Int. Sci.*, *16*, 182.
[10] Dane, K. Y., Nembrini, C., Tomei, A. A., Ehy, J. K., O'Neil, C. P., Velluto, D., Swartz, M. A., Inverandi, L., & Hubbell, J. A. (2011). *J. Contr. Release*, *156*, 154–160.
[11] Zheltonozhskaya, T., Nedashkovskaya, V., Khutoryanskiy, V., Gomza, Yu., Fedorchuk, S., Klepko, V., & Partsevskaya, S. (2011). *Mol. Cryst. Liq. Cryst.*, *536*, 380.
[12] Zheltonozhskaya, T. *et al.* (2009). In: *Hydrogen-Bonded Interpolymer Complexes: Formation, Structure and Applications*, Khutoryanskiy, V. V. & Staikos, G. (Eds), Chapter 5, World Scientific Publ. Co.: New Jersey-London-Singapore etc., 85.
[13] Zheltonozhskaya, T., Fedorchuk, S., & Syromyatnikov, V. (2007). *Russ. Chem. Rev.*, *76*, 731.
[14] Khougaz, K., Gao, Z., & Eisenberg, A. (1994). *Macromolecules*, *27*, 6341.
[15] Ali, H. S. M., York, P., Blagden, N., Soitanpour, S., Acree, W. E., & Jouyban, Jr. and A. (2010). *J. Chem. Eng. Data*, *55*, 578.
[16] Li, X.-S., Wang, J.-X., Shen, Z.-G., Zhang, P.-Y., Chen, J.-F., & Yun, J. (2007). *Int. J. Pharm.*, *342*, 26.